AJNR

MR Imaging-Related Heating of Deep Brain Stimulation Electrodes: In Vitro Study

Daniel A. Finelli, Ali R. Rezai, Paul M. Ruggieri, Jean A. Tkach, John A. Nyenhuis, Greg Hrdlicka, Ashwini Sharan, Jorge Gonzalez-Martinez, Paul H. Stypulkowski and Frank G. Shellock

AJNR Am J Neuroradiol 2002, 23 (10) 1795-1802
http://www.ajnr.org/content/23/10/1795

AJNR Am J Neuroradiol 23:1795–1802, November/December 2002

MR Imaging-Related Heating of Deep Brain Stimulation Electrodes: In Vitro Study

Daniel A. Finelli, Ali R. Rezai, Paul M. Ruggieri, Jean A. Tkach, John A. Nyenhuis, Greg Hrdlicka, Ashwini Sharan, Jorge Gonzalez-Martinez, Paul H. Stypulkowski, and Frank G. Shellock

BACKGROUND AND PURPOSE: **Recent work has shown a potential for excessive heating of deep brain stimulation electrodes during MR imaging. This in vitro study investigates the relationship between electrode heating and the specific absorption rate (SAR) of several MR images.**

METHODS: **In vitro testing was performed by using a 1.5-T MR imaging system and a head transmit-receive coil, with bilateral deep brain stimulation systems positioned in a gel saline-filled phantom, and temperature monitoring with a fluoroptic thermometry system. Standardized fast spin-echo sequences were performed over a range of high, medium, and low SAR values. Several additional, clinically important MR imaging techniques, including 3D magnetization prepared rapid acquisition gradient-echo imaging, echo-planar imaging, quantitative magnetization transfer imaging, and magnetization transfer-suppressed MR angiography, were also tested by using typical parameters.**

RESULTS: **A significant, highly linear relationship between SAR and electrode heating was found, with the temperature elevation being approximately 0.9 times the local SAR value. Minor temperature elevations, <1°C, were found with the fast spin-echo, magnetization prepared rapid acquisition gradient-echo, and echo-planar clinical imaging sequences. The high dB/dt echo-planar imaging sequence had no significant heating independent of SAR considerations. Sequences with magnetization transfer pulses produced temperature elevations in the 1.0 to 2.0°C range, which was less than theoretically predicted for the relatively high SAR values.**

CONCLUSION: **A potential exists for excessive MR imaging-related heating in patients with deep brain stimulation electrodes; however, the temperature increases are linearly related to SAR values. Clinical imaging sequences that are associated with tolerable temperature elevations in the ≤2.0°C range at the electrode tips can be performed safely within an SAR range <2.4 W/kg local (0.9 W/kg whole body averaged).**

Deep brain stimulation (DBS) treatment of refractory movement disorders and other conditions is a rapidly evolving neurosurgical field, with an ever increasing number of patients undergoing DBS surgery for Parkinson disease, essential tremor, dystonias, epilepsy, and obsessive compulsive disorders (1, 2). MR imaging is integral to evaluation and surgical planning for patients considered for DBS surgery and is also of critical importance in ongoing management. MR imaging may be required in several clinical scenarios, including verification of lead position; evaluation of patients with poor or worsening outcomes of DBS; adverse side effects of DBS placement, with which precise localization of the electrode contact plate with respect to the target needs to be confirmed; the need to replace electrodes or place contralateral electrodes; and the need to evaluate other pathologic abnormalities related or unrelated to the DBS electrodes, including stroke, tumor, or hemorrhage (1–6). Presently, the only neurostimulation system for DBS that is approved by the Food and Drug Administration is labeled non-MR imaging compatible. It is recommended that patients with neurostimulation systems not undergo MR imaging examinations be-

Received February 4, 2002; accepted after revision July 16.

Supported by an unrestricted research grant from Medtronic, Inc., Minneapolis, MN.

From the Division of Radiology (D.A.F., P.M.R., J.A.T.), Neuroradiology Section, and the Division of Surgery (A.R.R., A.S., J.G.-M.), Section of Stereotactic and Functional Neurosurgery, The Cleveland Clinic Foundation, Cleveland, OH; the Department of Computer and Electrical Engineering (J.A.N.), Purdue University, West Lafayette, IN; Medtronic, Inc. (G.H., P.H.S.), Minneapolis, MN; and Keck School of Medicine (F.G.S.), Los Angeles, CA.

Address reprint requests to Daniel A. Finelli, MD, Section of Neuroradiology/L10, The Cleveland Clinic Foundation, 9500 Euclid Avenue, Cleveland, OH 44195.

cause of the potential for serious risks, including movement or dislodgement of the leads, excessive MR imaging-related heating, induced electrical currents, and functional disruption of the operational aspects of the device.

Previous MR imaging safety studies conducted on other electronically activated devices, such as cardiac pacemakers, have generally recommended strict prohibition of patients with electronically active devices from undergoing MR imaging (7–13). However, several recent studies have shown minimal risks associated with MR imaging of patients with bone fusion stimulators, some infusion pumps, and certain other implants (9, 13–18). Before performing MR imaging safety studies for patients with DBS implants, it is essential to collect in vitro experimental data to initially define MR imaging conditions that may permit imaging of patients to be performed safely. From an MR imaging safety consideration, the greatest concern for electronically activated or electrically conductive implants in the brain is excessive MR imaging-related heating, which can cause irreversible tissue damage (19–23). There have been reports of serious brain injuries in two patients with DBS systems: one who received RF diathermy treatments for an unrelated condition and one who was cardioverted for atrial fibrillation (24, 25). Thus, there is a very real potential for injury due to excessive MR imaging-related heating.

Recent work has shown that the electrode configuration, the type of RF coil, and the specific absorption rate (SAR) of the MR image are factors that strongly influence the local temperature increases at the electrodes (26). Brain imaging with a head transmit-receive coil efficiently couples applied RF energy to the target tissue. Although the local RF deposition and resultant SAR (the mass normalized rate at which RF energy is coupled to tissue) can be high, there is a much lower whole body averaged SAR than one would observe with a corresponding image in a body coil transmit-head coil receive design. Using a head transmit-receive coil, a considerable length of the conducting leads and the implantable pulse generator are outside the RF field, and this coil configuration has been shown to be associated with less RF-related heating than with a body coil transmit design in a previous study (26). The purpose of the present study was to assess in vitro the MR imaging-related heating effects of several clinically important MR imaging techniques, including fast spin-echo imaging, echo-planar imaging, magnetization prepared rapid acquisition gradient-echo imaging, quantitative magnetization transfer imaging, and MR angiography with magnetization transfer background suppression, when using a head transmit-receive coil design and a commercial 1.5-T system.

Methods

In Vitro Model

In vitro testing was performed on a 1.5-T MR imaging system (Vision software, version Numaris 3.0; Siemens Medical Systems, Iselin, NJ) with a head transmit-receive coil. A special Plexiglas phantom designed to approximate the size and shape of the human head and torso was developed and filled with a semi-solid aqueous gel prepared to simulate the electrical conductivity and thermal convection properties of tissue (26). The weight of the filled phantom is 70 lb and is the weight entered at registration for purposes of SAR calculation. A plastic grid frame with adjustable posts was placed at the bottom of the phantom to allow consistent positioning and support of the neurostimulators, extensions, and leads within the phantom (Fig 1). Currently, the only Food and Drug Administration-approved device for chronic DBS is the Activa Tremor Control System (Medtronic, Inc., Minneapolis MN). This neurostimulation system includes the model 7426 Soletra implantable pulse generator, the model 7495 quadripolar extensions, and models 3387 and 3389 DBS leads. In this study, we positioned bilateral DBS electrodes, extensions, and implantable pulse generators in a manner to emulate the clinical method of subcutaneous pectoral placement of the implantable pulse generators and subcutaneous extension from the implantable pulse generator up the chest, along the neck, and over the cranial convexity to connect with the electrode lead, which passes through the cerebral cortex, with electrode contact plates in the subthalamic region (Fig 2). The length of the DBS lead is 40 cm, and it is insulated along its entire length, except for the connector and the four contact plates in the distal 10 mm of the lead. It is desirable to keep the extension connector in a stable, nonmoving position at the level of the cranium and not in the neck. Therefore, it is the most common current clinical practice to loop the excess electrode lead around the burr hole and then connect to the extension. Similarly, the extensions are 51 cm. Frequently, excess length is looped around the perimeter of the implantable pulse generator. A previous study (26) showed that this was the configuration that produced the greatest temperature elevations when using the head transmit-receive coil. In that same study, the worst case scenario was to use the body transmit coil and take the entire excess length of electrode and extension and coil it in the pocket of the implantable pulse generator (26), a configuration that was associated with $\leq$25.3°C elevation in temperature (at 3.9 W/kg whole body averaged SAR). Thus, for these in vitro experiments, one lead (right) was configured in the typical, worst case configuration for head transmit-receive coils and one lead (left) was configured in the worst case configuration based on body transmit coils, for simultaneous heating tests. The electrodes are positioned parallel and coronally coplanar, spaced 3 cm apart. Each electrode system is electronically isolated, and pilot studies of unilateral versus bilateral placements have shown no interdependence for bilateral electrodes in these and several other electrode configurations.

Thermometry System and Placement of Temperature Probes

Temperature monitoring was performed at multiple locations by using an MR imaging-compatible fluoroptic thermometry system (Model 790; Luxtron, Santa Clara, CA). Previous studies and our own pilot work have confirmed that the maximum MR imaging-related heating of the electrodes occurs at the tip of the electrode, in the contact plate region (26). Four fluoroptic thermometry probes were used for simultaneous temperature recordings as follows: 1) right lead probe positioned within 0.1 mm above the contact plates of the distal right DBS electrode, 2) left lead probe positioned within 0.1 mm above the contact plates of the distal left DBS electrode, 3) middle probe positioned in between the distal right and left electrode tips (1.5 cm equidistant from the right and left electrodes), and 4) reference probe positioned remotely from the DBS electrodes within 1 cm of the edge of the head portion of the phantom.

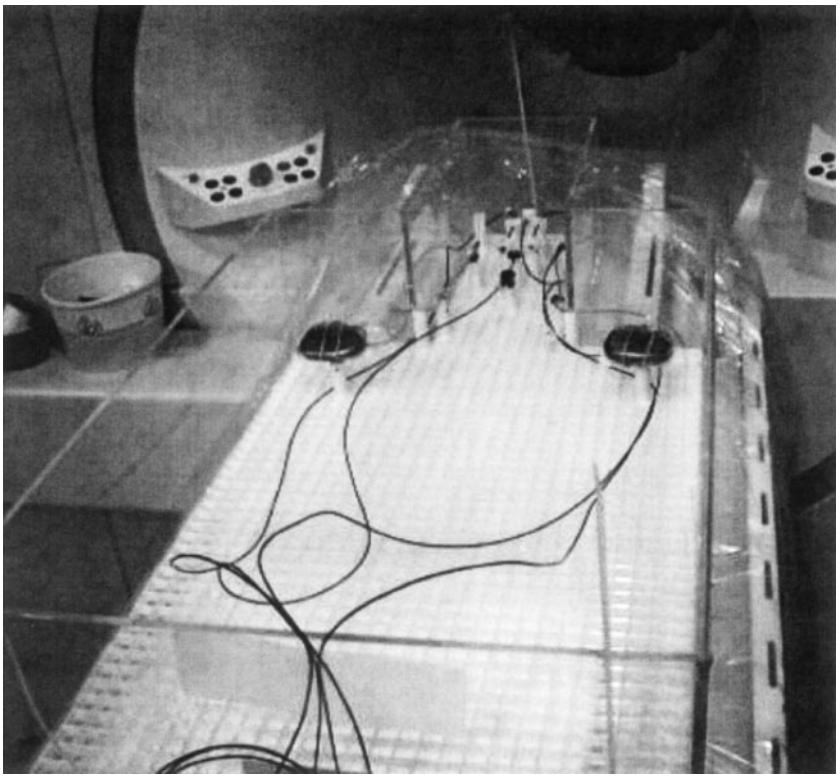

FIG 1. Phantom and experimental setup. Photograph shows the plexiglass phantom before filling with the gel saline solution shows the plastic grid frame and adjustable posts, which allow precise positioning and support of the dual implantable pulse generators, extensions, and DBS leads. The cables for the four fluoroptic thermometry probes are seen coursing off the bottom of the photograph.

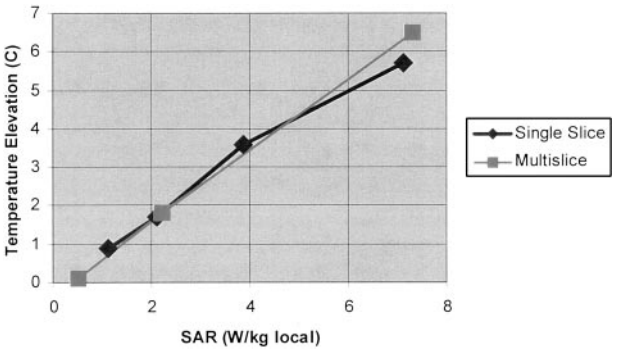

FIG 2. DBS lead mean temperature elevation as a function of local SAR. Plot shows greatest observed mean temperature elevation for 1 min of data collection, obtained at the time of peak heating during the 10- to 15-minute imaging time interval, versus local SAR value for single and multisection fast spin-echo images. Linear regression (all data points): $r = 0.994$, $P < .001$, x variable = 0.88, and y intercept = −0.13.

MR Imaging Sequences

To analyze the relationship between SAR and MR imaging-related heating of DBS electrodes when using the head coil transmit-receive architecture, we initially performed measurements by using a single section fast spin-echo sequence, positioned on the electrode tips, in which the RF amplitudes of the refocusing pulses were modulated to produce a range of low, medium, and high SAR values. Like most clinical MR imaging systems, this system estimates the whole body, partial body, and local SAR from the MR imaging parameters, the transmitter adjustments, and the patient weight entered at registration. Four measurements were performed over the SAR range from 1.12 W/kg local (0.04 W/kg whole body averaged) to 7.13 W/kg local (0.24 W/kg whole body averaged). Each measurement lasted 15 minutes. We then conducted identical tests by using an 18-section fast spin-echo sequence at three different SAR values: 0.5 W/kg local (0.02 W/kg whole body averaged), 2.17 W/kg local (0.07 W/kg whole body averaged), and 7.26 W/kg (0.24 W/kg whole body averaged). The mean and peak temperature elevations for both electrode leads and for the reference probes were recorded and were analyzed as a function of SAR.

Several routine, clinical MR imaging sequences were then tested with typical multisection or whole volume parameters, including T2-weighted fast spin-echo MR imaging (4000/120 [TR/effective TE]; echo train length, 7; local SAR, 0.5 W/kg; [0.02 W/kg whole body averaged]); echo-planar imaging (2000/65; local SAR, 0.14 W/kg; [0.01 W/kg whole body averaged]); magnetization prepared rapid acquisition gradient-echo imaging (11/3.9; local SAR, 0.36 W/kg; [0.01 W/kg whole body averaged]); quantitative magnetization transfer imaging (35/4.5, 10; magnetization transfer pulse, 700 degrees; off resonance, 3500 Hz; SAR, 3.4 W/kg local [0.11 W/kg whole body averaged]); and magnetization transfer-suppressed MR angiography (32/6.9, 7; magnetization transfer pulse, 500 degrees; off resonance, 1500 Hz; local SAR, 4 .28 W/kg; [0.14 W/kg whole body averaged]). These sequences were performed with multiple averages to achieve a 15-min measurement. The mean and peak temperature elevations for both electrode leads and for the reference probes were recorded and analyzed as a function of SAR.

Experimental Protocol

The neurostimulators, extensions, and electrodes were positioned in the phantom and fixed into place by using the grid and post system described previously. Fluorometry probes were then positioned as detailed above and were fixed with 4.0 silk sutures, away from the electrode contact plates and tips of the thermometry probes. The gel saline solution was then placed in the phantom and filled to a level of approximately 9 to 10 cm, completely covering all components. The gel was prepared in the ambient environment of the MR imaging work area several hours previously and was kept in sealed, airtight containers. We then allowed at least 30 minutes for equilibration of the system to the ambient conditions within the MR imager itself before beginning measurements. After recording baseline tempera-

TABLE 1: Deep brain stimulation temperature measurements

Sequence	SAR (W/kg)		Temperature (°C)		ΔT_{mean} (°C)	ΔT_{max} (°C)	$P < .01$
	Local	Whole Body	Baseline	Imaging			
Standardized sequence							
FSE SS	7.13	0.24	24.8 ± 0.1	30.5 ± 0.1	5.7	5.8	*
FSE SS	3.87	0.13	24.6 ± 0.2	28.2 ± 0.1	3.6	3.7	*
FSE SS	2.10	0.07	24.4 ± 0.1	26.1 ± 0.1	1.7	2.3	*
FSE SS	1.12	0.04	24.9 ± 0.1	25.8 ± 0.2	0.9	1.3	*
FSE MS	7.26	0.24	24.8 ± 0.1	31.3 ± 0.1	6.5	6.7	*
FSE MS	2.17	0.07	24.8 ± 0.1	26.6 ± 0.1	1.8	2.0	*
FSE MS	0.50	0.02	24.1 ± 0.1	24.2 ± 0.1	0.1	0.3	
Clinical sequences							
EPI	0.14	0.00	23.7 ± 0.1	23.9 ± 0.1	0.2	0.3	
MPRAGE	0.36	0.01	23.3 ± 0.1	23.4 ± 0.1	0.1	0.2	
QMT	3.44	0.11	23.8 ± 0.1	24.8 ± 0.1	1.0	1.5	*
MT MRA	4.28	0.14	24.2 ± 0.1	25.8 ± 0.1	1.6	1.8	*

Note.—SAR indicates specific absorption rate; ΔT_{mean}, mean temperature increase; ΔT_{max}, maximum observed temperature increase; FSE, fast spin-echo; SS, single section; MS, multisection; EPI, echo-planar imaging; MPRAGE, magnetization prepared rapid acquisition gradient-echo; QMT, quantitative magnetization transfer; MT MRA, magnetization transfer-suppressed MR angiography. Baseline temperature is the mean ± 1 SD of 12 consecutive measurements (1 min of data) at ambient conditions before the start of the MR imaging sequence. Imaging temperature is the mean ± 1 SD of 12 consecutive measurements (1 min of data) obtained during 10 to 15 min of continuous imaging, encompassing the time of the maximum observed temperature increase. For all measurements, the background reference temperature increase was <0.5°C.

ture measurements for 1 minute at 5-second intervals, MR imaging measurement was begun and lasted for 15 minutes, with temperatures being recorded at 5-second intervals. When the imaging was completed, temperature monitoring was performed for at least 1 minute or until baseline ambient temperature readings were achieved in all probes. Subsequent MR imaging was then performed as outlined above.

Data Analysis

The temperature readings from the four thermometry probes were collected in a file, which was exported to an Excel spreadsheet (Microsoft Corporation, Redmond, WA). The temperature change was calculated by subtracting the baseline temperature from the temperature measured at each time point for each probe position. For the initial standardized measurements over the low to high SAR range, the 12 baseline samples obtained during the minute before beginning the measurement were compared with 12 samples (1 minute) at the time of maximum heating. A *t* test was used to determine the statistical significance of any observed temperature changes. The maximum and mean temperature elevations were recorded for each probe position. The relationship between SAR and the mean temperature elevation measured for the hottest DBS electrode was analyzed by using linear regression analysis.

Plots of temperature change versus time during MR imaging with the clinical imaging sequences were then constructed. Again, the 12 baseline samples obtained during the minute before beginning the measurement were compared with 12 samples (1 minute) at the time of maximum heating. The maximum and mean temperature elevations were determined in each probe position. A *t* test was used to determine the statistical significance of any observed mean temperature changes.

Results

The temperature elevations observed with the standardized fast spin-echo measurements over the range of SAR values are listed in the Table. We found virtually identical, highly linear, statistically significant relationships between the local averaged and whole body averaged SAR values and the observed temperature increase measured at the DBS electrode tips for the single section and multisection fast spin-echo sequences (Fig 2; linear regression, $r = 0.994$; $P < .001$; x variable = 0.88; y intercept = −0.13). A maximum temperature elevation of 6.7°C was observed with the sequence having a local SAR of 7 .3 W/kg (0.24 W/kg whole body averaged). The electrode configuration that was associated with the greatest MR imaging-related heating in the head transmit-receive coil was the right lead (excess lead coiled at the burr hole, excess extension coiled at the implantable pulse generator), confirming the findings of a previous study (26). By interpolation, the SAR values at which a 1°C temperature rise at the electrode tips is expected is approximately 1.2 W/kg local or approximately 0.045 W/kg whole body averaged and the SAR values at which a 2°C temperature rise at the electrode tips is expected is approximately 2.4 W/kg local or approximately 0.09 W/kg whole body averaged. The background temperature increase was <0.5°C for all measurements, even at high SAR values.

The temperature elevations observed with the clinical imaging sequences are shown in the Table. The fast spin-echo, echo-planar, and magnetization prepared rapid acquisition gradient-echo imaging sequences had local SAR values <0.5 W/kg. None of these clinical imaging sequences was associated with DBS electrode temperature elevations >0.5°C. The experimental temperature elevations observed with fast spin-echo, echo-planar, and magnetization prepared rapid acquisition gradient-echo imaging sequences were all within 0.1°C of that predicted by the regression analysis above. Therefore, this in vitro model indicates that fast spin-echo, echo-planar, and magnetization prepared rapid acquisition gradient-echo imaging sequences performed with typical pa-

rameters and within these SAR restrictions are associated with no significant MR imaging-related heating. The echo-planar imaging sequences, which have very low SAR values, showed no significant heating of the DBS electrodes above the reference probe, indicating that the high dB/dt associated with the echo-planar imaging sequence has no apparent heating effects independent of the SAR considerations.

Quantitative magnetization transfer imaging and magnetization transfer-suppressed MR angiography, with local SAR values of 3.4 and 4.3 W/kg, respectively, had temperature elevations of <2.0°C. Interestingly, the temperature elevations observed with both of these sequences, with which most the RF deposited in a long duration, off resonance magnetization transfer prepulse, was less than expected based on our previous results by using the standardized fast spin-echo sequences.

Discussion

MR imaging-related heating at the DBS electrode tips occurs when the RF field induces a current in the lead and extension wires and some of this induced current passes through the electrode contact plates and into the surrounding tissues. The temperature increase at the electrode contacts is proportional to the square of the emanating current. Because the SAR is proportional to the square of the induced electric field, it is expected, and this study confirmed, that a linear relationship exists between the SAR and the temperature elevation measured at the contact plates (7, 19). Regression analysis of the experimental data also confirmed the expectation that the *y* intercept should be essentially zero (ie, with no applied RF, there is no temperature elevation). It is important to recognize that the RF induction of current in the electrode lead is a very different phenomenon from what might be understood about RF excitation signal intensity generation in MR imaging. The current induced in the conductor depends mainly on its electrical conductivity properties, the length and configuration (loops) of the conductor in the primary RF field, its position in the primary RF field (there are inhomogeneities in the RF profile, especially adjacent to coil elements and in the periphery of the RF field), and the effective RF power. The application of a section-select gradient produces only a small change (a few hundred hertz) in the local carrier frequency of the RF (ie, the Larmor frequency, or 63.5 MHz for this study). This has no significant impact on the induction of current in the lead. When RF is applied, it is always through the entire sensitive volume of the transmit coil. Theoretically, there should be no significant dependence of the induced current in the lead (or resultant heating) on section-select events (ie, single section, multisection, nonselective, imaging orientation, positioning an imaging section on the lead or through the lead, etc.). The concordance of the single section-multisection fast spin-echo data reported herein supports these concepts about MR imaging-related heating of conductors.

The phantom design, sequence design, electrode lead positioning, and use of a physiological gel saline solution were chosen to emulate a worst case MR imaging-related heating scenario, in which MR imaging-related heating is maximized, thermal convection is constrained (compared with pure aqueous solutions), and no tissue perfusion occurs to carry away heat. Using this worst case scenario in our experimental design maintains a conservative approach to the inference of "safety" when performing certain MR imaging of patients with implanted DBS electrodes. Previous studies of RF and other thermal ablation techniques have shown that reversible thermal lesions occur when the local temperature is elevated to the 42 to 44°C range (a 5–7°C elevation over the normal body temperature of 37°C) and that irreversible thermal lesions occur when the local temperature is elevated above 45°C (>8°C elevation over normal body temperature) (27–30). Febrile illnesses associated with fever to the 40°C range are not associated with any evidence of neural tissue damage (31). Therefore, transient temperature elevations of 1 to 2°C for several minutes while undergoing MR imaging examinations are expected to be easily tolerated with no adverse physiological effects. As is evidenced in several recent articles about RF thermal ablation of liver lesions, local tissue perfusion has a dramatic effect on heat deposition (30, 32–36). Normal brain perfusion would diminish the temperature elevations associated with MR imaging compared with the results of this in vitro work; however, participant safety, experimental design issues with electrode and fluoroptic probe positioning, and research ethics preclude trying to perform in vivo testing of MR imaging-related heating associated with DBS electrodes in human study participants. An unpublished survey of functional neurosurgical investigators at a recent meeting indicates that, to date, several hundred MR imaging studies of patients with this particular neurostimulation system have been performed with no adverse events (A.R. Rezai, unpublished results). Thus, this in vitro work provides confirmation that conventional clinical MR imaging sequences of the brain, performed with a head transmit-receive coil, are associated with minimal, physiologically tolerable, safe temperature elevations at the DBS electrode tips.

A second mechanism by which an electrical current can be induced in a conductor is by fluctuating magnetic field gradients; therefore, there was some concern that the high dB/dt (approximately 70 T/s) echo-planar imaging sequences may be associated with some additional heating beyond that associated with RF transmission. We found this not to be the case; based on the local SAR for the echo-planar imaging sequence, we would have predicted a temperature elevation of 0.3°C, which was exactly our measured result. Therefore, one can assume that for clinical MR imaging sequences, MR imaging-related heating is dependent only on RF electrical field induction of current in the leads.

A somewhat unanticipated result was that the temperature elevations associated with two MR imaging sequences using magnetization transfer were less than expected for their relatively high SAR values. Both of these magnetization transfer imaging methods use a long duration, high amplitude, off resonance magnetization transfer pulse. These results should be interpreted with extreme caution, because we expected to observe temperature elevations in the 4°C range based on the SAR values of the magnetization transfer imaging sequences, which would be unacceptable from an MR imaging safety standpoint. Although there are numerous magnetization transfer pulse parameters and tissue-specific issues that influence magnetization transfer imaging techniques (37–39), theoretically, there should be no significant dependence of the amount of induced current in the electrode lead related to the magnetization transfer pulses being a few kilohertz off resonance. Likewise, the RF profile of the head coil is not going to change because the transmitted RF is off resonance. Calculations of SAR values may be different for various manufacturers and models and may even be dependent on the specific RF pulses used in a particular sequence. The MR imaging system used in this trial does not make any modifications of SAR calculations based on tissue distributions or based on the magnetization transfer pulses being off resonance or having slightly different tissue RF absorption. Its SAR calculations are based on the summation of the time integrals of the RF pulses, the sequence TR, and the entered patient weight. The most likely explanation for the less-than-expected observed heating with the magnetization transfer imaging sequences relates to the MR system being an older clinical imaging system that uses an RF amplifier with tubes, not solid state circuitry. For the long duration, high amplitude magnetization transfer pulses, which have flip angle equivalents of 700 to 1200 degrees, the RF amplifier cannot maintain the voltage necessary for the high RF output and powers down to prevent tube overload. Thus, with these magnetization transfer imaging sequences, the machine is not actually transmitting the full RF power that the SAR calculation would represent. This hardware-related phenomenon is likely to be machine, model, and even individual imager specific and will likely vary over the life of the RF amplifier tubes. This effect will be magnetization transfer imaging sequence dependent and is also likely to be patient dependent, varying with the loading of the coil, because transmitter adjustments will determine how much voltage is needed to produce 90, 180, and all other degree RF pulses. Therefore, a great deal of uncertainty exists with respect to accepting as representative the apparently minor temperature elevations (1.5–1.8°C) seen with the quantitative magnetization transfer and magnetization transfer-suppressed MR angiography sequences. Most clinical quantitative magnetization transfer imaging sequence techniques are designed to have moderately high SAR values, in the 3.0 to 4.0 W/kg local SAR range or higher, because increasing the effective magnetization transfer power increases the dynamic range of the magnetization transfer ratio values (37). It is expected that maintaining SAR values of approximately 2.0 W/kg local with the magnetization transfer imaging sequences would be associated with minor, tolerable temperature elevations, but we have not performed these confirmatory experiments. Therefore, in keeping with a conservative approach to MR imaging safety, we recommend avoiding sequences using magnetization transfer imaging for patients with neurostimulation systems until more detailed testing resolves these uncertainties.

We have shown that MR imaging-related heating for fast spin-echo, gradient-echo, and echo-planar imaging sequences (and, by implication, for conventional spin-echo sequences as well) in the head transmit-receive coil is linearly correlated with SAR and that sequences performed within the prescribed SAR range of $\leq$2.4 W/kg local (0.09 W/kg whole body averaged) should be safe from a standpoint of MR imaging-related heating. This is a very important result from the standpoint of potential clinical imaging scenarios for patients with DBS electrodes. It is possible to safely obtain high resolution stereotactic 3D gradient-echo images and T2-weighted fast spin-echo images for documenting electrode contact plate positioning in patients with poor or worsening response to DBS and for placement of additional DBS electrodes. MR images to evaluate tumors and strokes, contrast-enhanced images, diffusion- and perfusion-weighted images, and non-magnetization transfer MR angiograms can all be safely obtained. Perhaps most importantly for future neuroimaging research in the functional and restorative neuroscience field, functional MR imaging studies can be performed safely from an MR imaging-related heating standpoint. It is acknowledged that other specific clinical sequences may ordinarily be performed with SAR values above the suggested limits, but simply prolonging the TR appropriately should allow these to be performed safely for patients with DBS electrodes.

There are several other MR imaging safety issues that were not addressed in this investigation, such as inappropriate neural stimulation, dislodgement-translation of the device by the static magnetic field, and disruption of the functional integrity of components. In general, previous studies have shown that if the implantable pulse generator is programmed to "off" and the voltage is set to 0 volts, no electrical stimulation occurs and the device is not damaged (1). Static magnetic field interactions, such as displacement or torque of the leads, are a subject of current investigation.

Food and Drug Administration guidelines (1998) define MR imaging operating conditions that may pose significant risk to patients. For RF energy, significant risk exposures are associated with an SAR $>$4.0 W/kg whole body for 15 min, 3.0 W/kg averaged over the head for 10 minutes, 8.0 W/kg in any gram of tissue in the head or torso for 15 minutes, or 12 W/kg in any gram of tissue in the extremities for 15 minutes (7, 11, 40). It is important to recognize that our

recommendations for safe RF exposures in patients with DBS electrodes (<2.4 W/kg local SAR over the head, 0.09 W/kg whole body averaged) are stricter than the current Food and Drug Administration guidelines and apply only to imaging of the brain with a head transmit-receive coil. Previous Food and Drug Administration guidelines (12) had considered there to be no significant risk associated with RF exposure when MR imaging produced <1°C measured temperature elevation in various body parts or skin surfaces. In this manner, brain MR imaging with head transmit-receive coils in patients with implanted DBS electrodes should pose no significant risk with local SAR values <1.2 W/kg (0.045 W/kg whole body averaged). Minor, physiologically tolerable, safe temperature elevations in the 1 to 2°C range are expected with local SAR values ≤2.4 W/kg (0.09 W/kg whole body averaged).

MR imaging safety guidelines for patients with DBS systems who are undergoing imaging of the brain have been developed (26). This current in vitro study allows us to expound on some of the recommendations. The neurostimulation systems must be checked before imaging is performed and interrogated for proper performance of all components. There must be no broken electrode leads, connectors, or extensions. The amplitude for each neurostimulation system must be programmed to 0 volts, and the output turned to off before entering the magnetic field environment. Thus far, the published data about imaging examinations of the brain concerns the use of 1.5-T MR imaging systems only. The most thorough support for safety of various clinical MR imaging sequences is restricted to MR imaging systems with a head transmit-receive coil architecture. The safety of other MR imaging systems and other examinations in the body has not been established. With the head transmit-receive system, the local SAR should not exceed 2.4 W/kg (approximately 0.09 W/kg whole body averaged SAR) for any brain imaging sequences. Sequences should always be performed at the lowest possible SAR levels. It seems that most routine clinical imaging of the brain techniques may be safely performed within the above SAR restrictions, including fast spin-echo, spin-echo, gradient-echo, magnetization prepared rapid acquisition gradient-echo, echo-planar, diffusion, perfusion, and functional MR imaging. Quantitative magnetization transfer imaging techniques should be considered prohibited. MR angiographic techniques should not use magnetization transfer background suppression. Patients should be instructed to immediately report any unusual sensations that may occur during the MR imaging examination. Patients must be continuously monitored by visual and verbal means. Extreme caution is recommended concerning conscious sedation. After MR imaging is completed, the neurostimulation systems must be interrogated again to verify functionality and then reprogrammed to previous stimulation parameters.

Conclusion

In vitro testing suggests that many of the MR imaging sequences in our clinical imaging armamentarium can be performed safely in patients with DBS electrode implants by using head transmit-receive coils on 1.5-T MR imaging systems, with acceptable minor temperature elevations. There are complexities, variabilities, and uncertainties about predicting the MR imaging-related heating associated with quantitative magnetization transfer and magnetization transfer-suppressed MR angiography sequences, and it is recommended that magnetization transfer imaging techniques be avoided until more specific testing establishes safe parameters.

Acknowledgments

We thank Dr. Ralf Loeffler for his steadfast concern about maintaining a safe MR imaging environment for patients with DBS electrodes and Dr. Gregory C. Hurst for insights on the impact of magnetization transfer pulse parameters on electrode heating.

References

1. Rezai AR, Lozano AM, Crawley AP, et al. **Thalamic stimulation and functional magnetic resonance imaging: localization of cortical and subcortical activation with implanted electrodes.** *J Neurosurg* 1999;90:583–590
2. Zonenshayn M, Mogilner AY, Rezai AR. **Neurostimulation and functional brain stimulation.** *Neurol Res* 2000;22:318–325
3. Dormont D, Cornu P, Pidoux B, et al. **Chronic thalamic stimulation with three-dimensional MR stereotactic guidance.** *AJNR Am J Neuroradiol* 1997;18:1093–1097
4. diPierro CG, Francel PC, Jackson TR, Kamiryo T, Laws ER Jr. **Optimizing accuracy in magnetic resonance imaging-guided stereotaxis: a technique with validation based on the anterior commissure-posterior commissure line.** *J Neurosurg* 1999;90:94–100
5. Mobin F, De Salles AA, Behnke EJ, Frysinger R. **Correlation between MRI-based stereotactic thalamic deep brain stimulation electrode placement, macroelectrode stimulation, and clinical response to tremor control.** *Stereotact Funct Neurosurg* 1999;72:225–232
6. Limousin P, Krack P, Pollak P, et al. **Electrical stimulation of the subthalamic nucleus in advanced Parkinson's disease.** *N Engl J Med* 1998;339:1105–1111
7. Schaefer DJ. **Health effects and safety of radiofrequency power deposition associated with magnetic resonance procedures.** In: Shellock FG, ed: *Magnetic Resonance: Health Effects and Safety.* Boca Raton: CRC Press; 2001
8. Shellock FG. *Pocket Guide to Metallic Implants and MR Procedures: Update 2001.* New York: Lippincott-Raven Healthcare; 2001
9. Shellock FG. **MR imaging and electronically activated devices [letter].** *Radiology* 2001;219:294–295
10. Hayes DL, Holmes DR Jr, Gray JE. **Effect of a 1.5 tesla magnetic resonance imaging scanner on implanted permanent pacemakers.** *J Am Coll Cardiol* 1987;10:782–786
11. Zaremba L. **FDA guidance for MR system safety and patient exposures: current status and future considerations.** In: Shellock FG, ed: *Magnetic Resonance Procedures: Health Effects and Safety.* Boca Raton: CRC Press; 2001:183–196
12. Food and Drug Administration. **Magnetic resonance diagnostic device: panel recommendation and report on petitions for MR reclassification.** *Fed Regist* 1988;53:7575–7579
13. Gangarosa RE, Minnis JE, Nobbe J, Praschan D, Genberg RW. **Operational safety issues in MRI.** *Magn Reson Imaging* 1987;5:287–292
14. Chou C-K, McDougall JA, Chan KW. **Absence of radiofrequency heating from auditory implants during magnetic resonance imaging.** *Bioelectromagnetics* 1995;16:307–316
15. Chou C-K, McDougall JA, Chan KW. **RF heating of implanted spinal fusion stimulator during magnetic resonance imaging.** *IEEE Trans Biomed Eng* 1997;44:367–372

16. Gleason CA, Kaula NF, Hricak H, et al. **The effect of magnetic resonance imagers on implanted neurostimulators.** *Pacing Clin Electrophysiol* 1992;15:81–94
17. Heller JW, Brackman DE, Tucci DL, Nyenhuis JA, Chou H-K. **Evaluation of MRI compatibility of the modified nucleus multichannel auditory brainstem and cochlear implants.** *Am J Otol* 1996;17:724
18. Liem LA, van Dongen VC. **Magnetic resonance imaging and spinal cord stimulation systems.** *Pain* 1997;70:95–97
19. Nyenhuis JA, Kildishev AV, Foster KS, Graber G, Athey W. **Heating near implanted medical devices by the MRI RF-magnetic field.** *IEEE Trans Magn* 1999;35:4133–4135
20. Schueler BA, Parrish TB, Lin JC, et al. **MRI compatibility and visibility assessment of implantable medical devices.** *J Magn Reson Imaging* 1999;10:596–603
21. New PF, Rosen BR, Brady TJ, et al. **Potential hazards and artifacts of ferromagnetic and nonferromagnetic surgical and dental materials and devices in nuclear magnetic resonance imaging.** *Radiology* 1983;147:139–148
22. Nyenhuis JA, Bourland JD, Kildishev AV, Schaefer DJ. **Health effects and safety of intense MRI gradient fields.** In: Shellock FG, ed: *Magnetic Resonance Procedures: Health Effects and Safety.* Boca Raton: CRC Press; 2001:31–54
23. Sawyer-Glover A, Shellock FG. **Pre-MRI procedure screening: recommendations and safety considerations for biomedical implants and devices.** *J Magn Reson Imaging* 2000;12:92–106
24. Nutt JG, Anderson VC, Peacock JH, Hammerstad JP, Burchiel KJ. **DBS and diathermy interactions induces severe CNS damage.** *Neurology* 2001;56:1384–1386
25. Yamamoto T, Katayama Y, Fukaya C, et al. **Thalamotomy caused by cardioversion in a patient treated with deep brain stimulation.** *Stereotact Funct Neurosurg* 2000;74:73–82
26. Rezai AR, Finelli DA, Nyenhuis JA, et al. **Neurostimulation systems for deep brain stimulation: in vitro evaluation of MRI-related heating at 1.5 T.** *J Magn Reson Imaging* 2002;15:241–250
27. Bligh J. *Temperature Regulation in Mammals and Other Vertebrates.* New York: American Elsevier; 1973:80–84
28. Heistad DD, Abboud FM. **Factors that influence blood flow in skeletal muscle and skin.** *Anesthesiology* 1974;41:139–156
29. Houdas Y, Ring EF. **Temperature distribution.** In: *Human Body Temperature: Its Measurements and Distribution.* New York: Plenum; 1982
30. Cosman ER. **Radiofrequency lesions.** In: Gildenberg PL, Tasker RR, eds: *Textbook of Stereotactic and Functional Neurosurgery.* New York: McGraw-Hill; 1992:973–985
31. Petersdorf RG. **Alterations in body temperature.** In: *Harrison's Principles of Internal Medicine.* 10th ed. New York: McGraw-Hill; 1983:50–57
32. Chua E, Gose E, Vinas FC, Dujovny M, Star J. **Temperature distribution produced in brain tissue and other media by a radiofrequency hyperthermia generator.** *Stereotact Funct Neurosurg* 1999;72:22–34
33. Jain MK, Wolf PD. **A three-dimensional finite element model of radiofrequency ablation with blood flow and its experimental validation.** *Ann Biomed Eng* 2000;28:1075–1084
34. Gazelle GS, Goldberg SN, Solbiati L, Livraghi T. **Tumor ablation with radiofrequency energy.** *Radiology* 2000;217:633–646
35. Goldberg SN, Hahn PF, Halpern EF, Fogle RM, Gazelle GS. **Radiofrequency tissue ablation: effect of pharmacologic modulation of blood flow on coagulation diameter.** *Radiology* 1998;209:761–767
36. Anzai T, Lufkin R, DeSalles A, Hamilton DR, Farahani K, Black KL. **Preliminary experience with MR-guided thermal ablation of brain tumors.** *AJNR Am J Neuroradiol* 1995;16:39–48
37. Finelli DA. **Magnetization transfer in neuroimaging.** *Magn Reson Imaging Clin N Am* 1998;6:31–52
38. Hua J, Hurst GC. **Analysis of on- and off-resonance magnetization transfer techniques.** *J Magn Reson Imaging* 1995;5:113–120
39. Grossman RI, Gomori JM, Ramer KN, et al. **Magnetization transfer: theory and clinical applications in neuroradiology.** *Radiographics* 1994;14:279–290
40. U.S.Food and Drug Administration, Center for Devices and Radiological Health. *Guidance for the submission of premarket notifications for magnetic resonance diagnostic devices.* 1998. Available on the FDA web site at http://www.fda.gov/cdrh/ode/95.html.